INVESTIGATING POTENTIAL COMFORT BENEFITS OF BIOLOGICALLY-INSPIRED BUILDING SKINS

Matthew Webb[1], Lu Aye[1], and Ray Green[2]
[1] Department of Infrastructure Engineering, University of Melbourne, Australia
[2] Faculty of Architecture, Building and Planning, University of Melbourne, Australia

ABSTRACT

Biomimicry offers opportunities to advance the development of flexible building facades. Here, the combination of external fur, bioheat transfer (blood perfusion) and internal surface evaporation are combined into a model of a commercial office building façade. Temperatures and heat transfer are calculated in a dynamic simulation for summer conditions in a temperate climate (Melbourne, Australia). Thermal comfort, in terms of PMV and PPD, is assessed and compared to a reference case.

Keywords: biomimicry, adaption, façade, thermal comfort, bioheat transfer.

INTRODUCTION

Humans have evolved an effective, efficient thermoregulation system and are able to survive (and thrive) in widely varying climates. They interact with their thermal environment through three modes of heat transfer – conduction, convection and radiation.

Skin is a key component in human thermoregulation and acts as the heat transfer interface to the external thermal environment. If the brain's hypothalamus detects excessive heat gain, sweating begins, promoting evaporation. Hairs flatten against the skin, and warm blood flow to vessels beneath the skin surface (vasodilation) maximises radiant heat transfer.

The goal of this study was to determine if the characteristics of human skin, when translated via systematic biomimicry into the technological domain, could act to improve thermal performance and improve occupant thermal comfort. A representative façade 'skin' model was derived to analyse heat transfer in a summer cooling scenario and compared to a conventional static façade.

Heat Transfer in living tissue – Bioheat Transfer

Heat transfer in living tissue has been studied for more than a century (Charny 1992, p19). Perhaps the greatest advancement in the field came with the research of Pennes (1948), who modelled heat transfer in the resting human forearm. Pennes' main aim was to ascertain the relationship between arterial blood flow and tissue temperature. Pennes (1948, p116) assumed that this heat transfer depended upon temperature difference between the artery, tissue and veins. Pennes based his model on the law of conservation of energy. He allowed for metabolic heat production via a constant term (q'''_m) and also accounted for the heat transferred through blood perfusion ($\dot{w}_b$, in $m^3/m^3/s$) from arterial blood into the tissues. Pennes' equation is as follows:

$$\rho_t c_{p,t} \frac{\partial T}{\partial t} = k_t \nabla^2 T + \rho_b c_{p,b} \dot{w}_b \left(T_{a0} - T\right) + q'''_m \quad (1)$$

Here:

- T is the tissue temperature,
- ρ_t and ρ_b are tissue and blood densities, respectively,
- $c_{p,t}$ and $c_{p,b}$ are the tissue and blood specific heat capacities, respectively,
- k_t = tissue thermal conductivity,
- T_{a0} = arterial inlet temperature,
- q'''_m = volumetric metabolic heat production.

Wulff, assuming that blood flow and temperature gradients are in the same direction, altered the Pennes approach by introducing a directional blood enthalpy term that described the heat content of blood flowing with an average velocity (Charny 1992, p34). Klinger expanded Wulff's model (Charny, 1992, p36-37) by allowing for a non-uniform velocity field (represented by the vector **v**):

$$\rho_t c_{p,t} \frac{\partial T}{\partial t} = k_t \nabla^2 T - \rho_b c_{p,b} \mathbf{v} \cdot \nabla T + q'''_m \quad (2)$$

Weinbaum and Jiji extended the bioheat transfer model to incorporate three layers: a cutaneous (skin) layer, an intermediate layer and deep layer, which recognised the complexity of fluid flow and vascular architecture (Jiji 2009, p314).

Weinbuam et al. (1997) acknowledged the complexity and limitations of the Weinbaum and Jiji equations and developed the "s-Vessel Cylinder Model" (Jiji 2009, p323), which generalised the bioheat energy balance. This model assumed that thermal exchange in tissue occurs at the scale of "s-vessels" of 50-100μm (Weinbaum et al. 1997, p280). In this model, Weinbaum et al. (1997, p284) defined

a perfusion source term ΔT^*, which could then be applied to the Pennes bioheat equation:

$$\rho_t c_{p,t} \frac{\partial T}{\partial t} = \nabla \cdot k_t \nabla T + \rho_b c_{p,b} \dot{w}_b \Delta T^* \left(T_{a0} - T\right) + q'''_m \quad (3)$$

Fur Heat Transfer

The thermodynamic properties of fur have been the subject of several studies since 1950. Scholander et al. (1950) and Hammel (1955) experimentally determined fur insulation values, for example between ~1.3 m^2K/W (shrew) and ~0.18 m^2K/W (white fox).

As described by Webb, Hertzsch and Green (2011, p459), Cena and Monteith (1975) and Kowalkski and Mitchell (1979) developed models of fur heat transfer. However, the detailed methodology of Davis and Birkebak (1974) was found to be the most amenable for translation to the built environment.

In this model, the energy flux from (or to) the skin surface, q_f (W/m^2) was related to a temperature gradient, ΔT, and fur thickness layer, L_f, via an effective fur thermal conductivity, k_{eff}:

$$q_f = k_{eff} \frac{\Delta T}{L_f} \quad (4)$$

Equation 4 accounted for conductive and diffuse radiative heat transfer through fur in the absence of direct solar radiation.

Thermal conductivity through the fur was calculated perpendicular to the skin as k_y:

$$k_y = \left\{\left(\rho_{eff}/\rho_f\right)k_f + \left[1 - \left(\rho_{eff}/\rho_f\right)k_a\right]\right\}\cos^2\theta_f + k_p \sin^2\theta_f \quad (5)$$

where:

- k_f = fur and air thermal conductivity (W/mK),
- k_a = air thermal conductivity (W/mK),
- k_p = thermal conductivity orthogonal to hair direction (W/mK).
- ρ_f = fur (hair) mass density (kg/m^3),
- ρ_{eff} = effective fur coat mass density (kg/m^3),
- θ_f = angle between hair and normal to skin.

Geometric variables L_f and θ_f are illustrated in Figure 1.

The long-wave radiative component of the thermal conductivity for the fur coat (k_{rad}) was as follows:

$$k_{rad} = k_{r-y}\left[1 + \frac{F_1 N_f}{4F_2}\frac{T_{sk}^4 - T_{\infty,r}^4}{T^3 \Delta T}\right]_{\eta=1/2} \quad (6)$$

where:

- F_1 and F_2 describe the radiation emitted from the skin and the amount of radiation passing through the y plane due to emission and scattering (for detailed definitions of F_1 and F_2 see Davis and Birkebak 1974, p. 256),
- T_{sk} = skin temperature (K),
- $T_{\infty,r}$ = temperature of radiation sink (K),
- T = temperature at evaluation point in the fur (K),
- ΔT = temperature difference between skin surface and external fur surface (K),
- η = non-dimensional length perpendicular to skin, i.e. y/L_f.

Furthermore:

$$N_f = 4\left(\rho_{eff}/\rho\right)\varepsilon_f L_f / \left(\pi d_f\right) \quad (7)$$

$$k_{r-y} = \left(8\sigma T^3 L_f F_2\right) / \left(\pi N_f\right) \quad (8)$$

where:

- σ = Stefan-Boltzmann constant, 5.67×10^{-8} $Wm^{-2}K^{-4}$,
- N_f = effective optical thickness of the fur (Davis and Birkebak, 1974, p256),
- k_{r-y} = diffuse radiative conductivity (Davis and Birkebak, 1974, p257)
- d_f = hair diameter (assumed circular, in m),
- ε_f = fur emissivity.

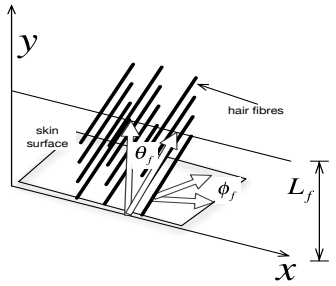

Figure 1 Basic geometry of fur model

Using k_y and k_{rad}, the effective thermal conductivity could be calculated as:

$$k_{eff} = k_y + k_{rad} \quad (9)$$

Heat transfer to/from the skin surface could then be calculated as per Equation 4.

Davis and Birkebak (1974, p260) then established a basis for heat transfer to/from a fur coat in the presence of direct solar radiation using the following equation:

$$q_f = \frac{k_{eff}}{L_f}\left(T_{s,e} - T_{f,e}\right) + \left(1 - \left[\cos\theta_s / \left(N_{f,s}F_s\right)\right]\right)q_{f,w} - \left(\alpha_{f,s} S \cos^2\theta_s / \left(N_{f,s}F_s\right)\right) \quad (10)$$

where:

- S = incident solar radiation (W/m^2),
- $\alpha_{f,s}$ = fur solar absorptivity,
- $N_{f,s}$ = effective optical thickness for solar wavelengths,
- $q_{f,w}$ = solar radiation absorbed by skin (W/m^2),

- F_s = absorption factor at solar wavelengths (Davis and Birkebak, 1974, p 259) ,
- $T_{f,e}$ = external fur temperature (K),
- $T_{s,e}$ = skin temperature (K, under fur layer).

Perspiration heat transfer

Several researchers have modelled perspiration heat transfer. Xu et al. (2009, p 10) cites two equations for heat loss from sweat evaporation from Wilson and Spence (1988) and Deng and Lui (2004).

Gebremedhin and Wu (2001) modelled evaporative cooling from a wet skin surface and fur layer. While based on bovines, the physical principles are equivalent to those for human skin. Furthermore, Gebremedhin and Wu parameterised their model in a way that can be readily transferred to façade design.

Gebremedhin and Wu (2001, p539) assumed a fur (δ_1) and an air (δ_2) boundary layer, such that the overall laminar diffusive zone is $\delta = \delta_1 + \delta_2$. Fick's law was used to describe the mass flux ($\dot{m}_{evap}$, kg/s) due to perspiration from the laminar boundary layer to the freestream:

$$\dot{m}_{evap} = \frac{\left(\rho_{s,i} - \rho_{a,i}\right)}{\frac{1}{h_{m,s,i}} + \frac{\delta}{D}} \qquad (11)$$

where:

- $\rho_{s,i}$ and $\rho_{a,i}$ are the mass concentrations of water vapour at the surface and in air, respectively (kg/m^3),
- D = vapour diffusion coefficient (m^2/s),
- $h_{m,s,i}$ = mass transfer coefficient (m/s).

The total evaporative heat transfer (q_{evap}, W/m^2) could then be calculated as:

$$q_{evap} = L_v \dot{m}_{evap} \psi_{\%} \qquad (12)$$

where:

- L_v = latent heat of evaporation of water (J/kg)
- $\psi_{\%}$ = percentage of wetted wall surface.

Sensible heat transfer (q_{sens}, W/m^2) was described by Gebremendhim and Wu (2001, p540) in terms of conduction through the fur layer, conduction in the laminar air layer and then convection only to the freestream. This led to:

$$q_{sens} = \frac{\left(T_{s,i} - T_{a,i}\right)}{\frac{1}{h_{c,s,i}} + \frac{\delta}{k_{s,i}}} \qquad (13)$$

where:

- $T_{s,i}$ and $T_{a,i}$ are the skin surface and air temperatures, respectively (K),
- $h_{c,s,i}$ = convective heat transfer coefficient from boundary layer to freestream (W/m^{2}K),
- $k_{s,i}$ = conduction heat transfer coefficient across the surface boundary layer, δ (W/mK).

Total heat transfer was the summation of the sensible and evaporative components:

$$q_{total} = q_{evap} + q_{sens} \qquad (14)$$

PROPOSED MODEL

An overall model was developed for an opaque building façade system that encompassed three biomimetic aspects:

- Exterior synthetic fur that interacts with the outdoor environment.
- Internal fluid perfusion that acts to cool (and heat) the façade.
- Interior perspiration evaporation surface that interacts with the internal room air.

Each of these components was combined into a single model as shown in Figure 2.

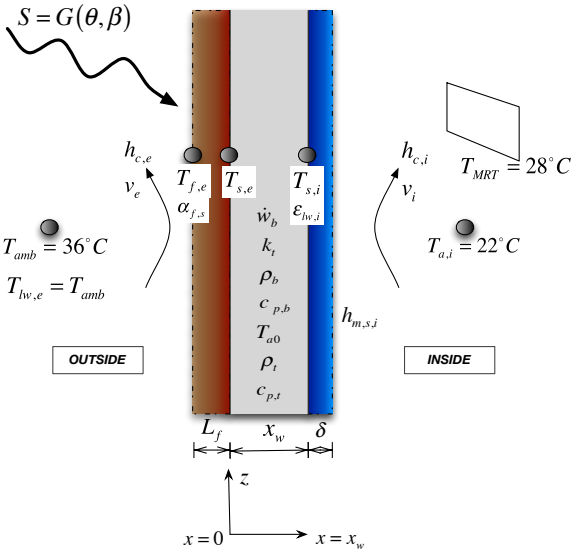

Figure 2 Proposed combination of fur, perfusion and evaporative layers

External fur layer

The physical model for the external fur layer was based upon Davis and Birkebak (1974). The key thermal parameter required was the effective thermal conductivity, k_{eff}, given by Equation 9 and repeated here:

$$k_{eff} = k_y + k_{rad} \qquad (15)$$

The heat transfer through the fur acts as an input, or boundary condition, to the perfusion layer.

Internal perfusion façade layer

For this paper we used a modified version of the Pennes bioheat equation to describe fluid perfusion through a unitised façade element. Firstly, this equation could be combined with the other elements in the model. Secondly, the proposed vascular architecture was generalised, composed of thermally significant minor vessels supplied from the major 'vessels' (i.e. hydronic pipework). We assumed that the cooling fluid was evenly distributed throughout

the façade. Thirdly, bulk fluid flow was orthogonal to the major temperature and heat gradients. Therefore, effects of fluid convection in the direction of major heat transfer were minimal. Effects of countercurrent heat exchange were assumed to be negligible. The model assumed a minimal temperature increase in the fluid through the façade element (1.0m wide, 0.1m thick). Hence a continuum model for perfusion was appropriate. We assumed no "metabolic" heat generation (no heat sources). Finally, we assumed that the physical properties of the fluid and façade were not temperature-dependent. The resultant Pennes perfusion bioheat equation to be used in the biomimetic model was as follows:

$$k_t \frac{\partial^2 T}{\partial x^2} + \rho_b c_{p,b} \dot{w}_b \left(T_{a0} - T\right) = \rho_t c_{p,t} \frac{\partial T}{\partial t} \qquad (16)$$

Interior perspiration layer

A similar evaporative model to that presented in Gebremendhim and Wu (2001) was developed to describe heat and mass transfer between the interior wall and room air. We assumed that the interior wall surface was smooth (i.e. without hair/fur layer). The key elements of this model to be incorporated into the combined façade model were the heat transfer components in Equations 12 and 13.

Combining the models

The three different components to the overall model were combined by applying the external fur layer and internal evaporative layer as boundary conditions to the solution of the time-dependent perfusion equation.

Heat transfer through the fur acted as an input to the internal perfusion layer. An equivalent calculation process to that presented in Webb, Hertzsch and Green (2011) was used. We assumed that the external short wave radiation (S), long wave radiation ($q_{radlw,e}$) and external convective heat transfer ($q_{conv,e}$) equalled the heat transfer through the fur (q_f). Hence:

$$S + q_{radlw,e} = q_{conv,e} + q_f \qquad (17)$$

Using h_{ce} as the external heat transfer coefficient (W/m^{2}K), $T_{s,e}$ as the external surface temperature (K) and T_{amb} as ambient temperature (K), Equation 17 could be rewritten as:

$$S + q_{radlw,e} = h_{c,e}\left(T_{s,e} - T_{amb}\right) + q_f \qquad (18)$$

The scheme for external radiation to built surfaces presented in CIBSE Guide J (Butcher 2002) was used for radiation calculations.

Noting that heat q_f flows through the fur to the external wall surface (i.e. underneath the fur layer):

$$q_f = -k_t \left.\frac{\partial T}{\partial x}\right|_{x=0} \qquad (19)$$

On the interior surface, the wetted surface of the perfusion façade interacted with the occupied space. Evaporative (q_{evap}), convective ($q_{conv,i}$), conductive ($q_{cond,bl}$) and long wave radiative ($q_{radlw,i}$) heat transfer were considered:

$$q_{sens} + q_{evap} + q_{radlw,i} = -k_t \left.\frac{\partial T}{\partial x}\right|_{x=x_w} \qquad (20)$$

Given the previous definitions for q_{evap} and q_{sens}, and using the method presented in Appendix 3.A3 of *CIBSE Guide A* (Butcher 1999) for internal long wave radiation exchange, the internal heat balance could be reformulated as:

$$\frac{\left(T_{s,i} - T_{a,i}\right)}{\frac{1}{h_{c,s,i}} + \frac{\delta}{k_{s,i}}} + L_v \psi_{\%} \frac{\left(\rho_{s,i} - \rho_{a,i}\right)}{\frac{1}{h_{m,s,i}} + \frac{\delta}{D}} + \left(\tfrac{6}{5}\right) 4\sigma T_{s,i}^3 E\left(T_{s,i} - T_{MRT}\right) = -k_t \left.\frac{\partial T}{\partial x}\right|_{x=x_w} \qquad (21)$$

Here, E is the Emissivity Factor (Butcher 1999, p3-37). In the simple case where the internal surfaces can be approximated by a cube (i.e. 6 internal surfaces of approximately the same area and emissivity, $\varepsilon_{lw,i} = \varepsilon_{2,lw} = 0.9$):

$$E = \varepsilon_{lw,i}\left[1 + \varepsilon_{lw,i}\left(1 - \varepsilon_{2,lw}\right)/5\varepsilon_{2,lw}\right]^{-1} \qquad (22)$$

Initially (at $t=0$) a linear temperature profile was assumed:

$$T(x,0) = 36 + \tfrac{22-36}{x_w} x \qquad (23)$$

SELECTION OF PARAMETERS

External fur layer

Webb, Hertzsch and Green (2011) optimised the physical parameters of a façade with an external fur layer. These parameters were used in the current analysis (Table 1).

Table 1
Outer fur layer properties

VARIABLE	SELECTED VALUE
L_f	$L_{f,\,summer} = 0.1$
d_f	0.0001
θ_f	60
n_f	12732395
ρ_{eff}/ρ_f	0.2
k_{eff}	0.055
$R_{TH,f}$	1.8
SOLAR PARAMETERS (EQUATION 10)	
$\theta_{f,s} = 60°$, $\alpha_{f,s} = 0.8$, $N_{f,s} = 124.3$, $F_s = 0.44$	

Internal perfusion façade layer

Internal façade properties were selected to be approximately equivalent to those of human biological tissue. Xu et al (2009, p8) showed that the thermal conductivity and specific heat of human blood are slightly lower than the properties of water, however water was the more practical option. In conventional cooling hydronic systems, water is generally supplied at a temperature of 287.15 K (Warma Floor, n.d.) to generate a surface temperature of 292-293 K (*Underfloor Heating/Cooling - Technical Information* n.d., p47).

This allows for meaningful heat exchange with the interal environment without causing condensation or thermal discomfort. Prevention of internal surface condensation is not a consideration in the case of the biomimetic façade. However, to maintain desired thermal comfort (*ASHRAE Handbook: Systems and Equipment* 2008, p6.11), and allow for comparison with a conventional hydronic system, the selected water supply temperature for the biomimetic facade was 287.15 K.

For the perfusion term, reference was made to the Pennes article (1948) and later reviews (Wissler, 1978, Charny, 1992). To correlate Pennes' model with experiemental results, Wissler (1978, p37), citing Barcroft and Edholm (1946), noted that a typical perfusion rate of 5.0 mL·100mL^{-1}·min^{-1}, or 5.0×10^{-4} m^3/m^3/s. With a façade width of 0.1 m and a porosity of 1% (99% solid 'tissue'), the cross sectional flow area is $0.1\times1\%=0.001$m^2 and the actual velocity is 0.05m/s.

The physical properties of the perfusion façade are summarised in Table 2 below.

Table 2
Perfusion façade physical properties

PARAMETER	SELECTED VALUE	UNITS
k_t	0.18	W/mK
ρ_b	998	kg/m^3
$c_{p,b}$	4180	J/kgK
$\dot{w}_b$	5.0×10^{-4}	m^3/ m^3/s
T_{a0}	287.15	K
q'''_m	0	W/m^3
ρ_t	495.3	kg/m^3
$c_{p,t}$	2300	J/kgK

Interior perspiration layer

For the internal façade wall we assumed that the surface was wetted by a percentage ψ = 90% and evaporative heat and mass transfer occurs over a distance δ (boundary layer thickness).

To calculate δ we used a similar combination of hydrodynamic and thermal principles as given in Gebremendhim and Wu (2001) for a cylinder and Holman (2001) for a flat plate. Holman (2001, p231) developed an expression for the boundary layer velocity, u, in terms of distance above the surface, y, and the freestream velocity, u_∞:

$$\frac{u}{u_\infty}=\frac{3}{2}\frac{y}{\delta}-\frac{1}{2}\left(\frac{y}{\delta}\right)^3 \qquad (24)$$

Holman (2001, p 246, 247) presented two equations for the average shear stress at the wall ($\bar{\tau}_w$):

$$\bar{\tau}_w=\bar{C}_f\rho_{air}\frac{u_\infty^2}{2};\ \tau_w=\mu\left.\frac{\partial u}{\partial y}\right|_w \qquad (25)$$

Here, μ was the air dynamic viscosity and ρ_{air} was the air density.

The velocity expression was differentiated and applied to the shear stress equation, and the two expressions for shear stress were combined to define an expression for δ in terms of the friction coefficient $\bar{C}_f$:

$$\delta=\frac{3\mu}{\bar{C}_f u_\infty} \qquad (26)$$

The friction coefficient itself was defined by the Stanton number, $\bar{\mathrm{St}}$, and Prandtl number, Pr, for air (Holman, 2001, p 246):

$$\bar{\mathrm{St}}\,\mathrm{Pr}^{2/3}=\bar{C}_f/2 \qquad (27)$$

Substituting the properties of air (evaluated at 300 K) to evaluate the hydrodynamic boundary layer thickness, δ was calculated as 5.88×10^{-3}m.

The diffusion coefficient D was calculated using the formula for water vapour in air (*ASHRAE Handbook: Fundamentals* 2005, p5.2):

$$D=\frac{0.926}{P}\left(\frac{T^{2.5}}{T+245}\right) \qquad (28)$$

The mass diffusion coefficient $h_{m,s,i}$ was calculated by using the correlation between heat and mass transfer (Holman, p 625) for flow over a flat plate. This led to $h_{m,s,i}=4.43\times10^{-3}$ m/s.

Finally, the latent heat of evaporation of water (L_v) was calculated using the formula presented in Henderson-Sellers (1983, p1188):

$$L_v=1.91846\times10^6\left(\frac{T_{a,i}}{T_{a,i}-33.91}\right)^2 \qquad (29)$$

SIMULATIONS

Heat transfer and comfort conditions for the proposed biomimetic façade 'skin' were tested in a cooling scenario simulation. Using the boundary conditions (Equations 19 and 21) plus the initial condition (Equation 23), the time dependent heat transfer given in Equation 16 could be solved using the Matlab numerical solver **pdepe**.

The simulation involved 3 connected parts:

- The outer fur layer,
- The perfusion layer (internal façade layer),
- The interior evaporative layer.

Equation 16 accounted for the façade's thermal mass and fluid perfusion. Through the boundary condition in Equation 19, the fur heat transfer, q_f, exerted influence on external surface of the perfusion façade. Similarly, the boundary condition in Equation 21 incorporated the effect of the internal evaporative layer.

In Matlab, the differential equation solver **pdepe** was included in a top level function. The equation form, boundary and initial conditions were written into a set of subfunctions, which also included the physical parameters as described in the previous section.

The simulation was conducted for typical summer conditions in Melbourne, Australia (see Table 3). Having defined the inputs, Equation 16 was solved numerically over a time period of 2 hours.

Table 3
Design test conditions

PARAMETER	SUMMER VALUE
T_{amb} (K)	309.15
Wind velocity, v_e (m/s)	2
Global irradiance G, (W/m^2)	800
Diffuse irradiance, D, (W/m^2)	400
Solar azimuth, α_s	45°
Solar altitude, γ_s	60°
Wall slope, β	90°
Internal air temperature, T_{ai} (K)	295.15
Mean radiant temperature, T_{MRT} (K)	301.15
Convection coefficient, $h_{c,i}$ (W/m^{2}K)	6

RESULTS

Figures 3 and 4 plot the temperature profile within the façade at the end of the simulation (i.e. t = 7200s). For comparison, façade temperatures are plotted against a reference wall without biomimetic initiatives. Heat transfer components from the internal surface of the façade are shown in Figure 5. Positive values indicate heat transferred *to* the occupied space.

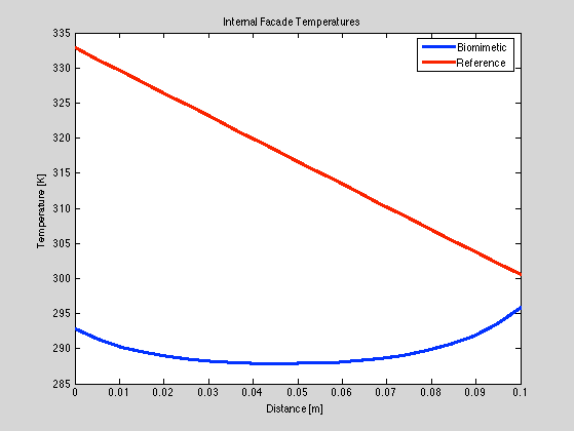

Figure 3 Temperature plots – biomimetic and reference models

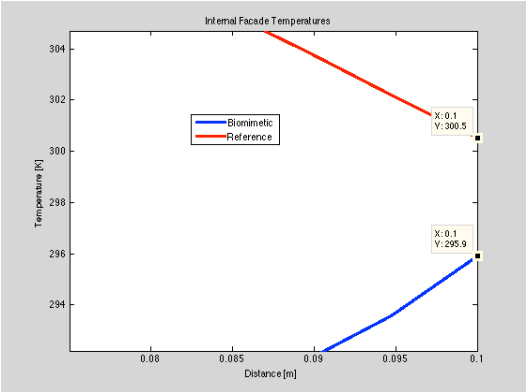

Figure 4 Inside surface temperatures

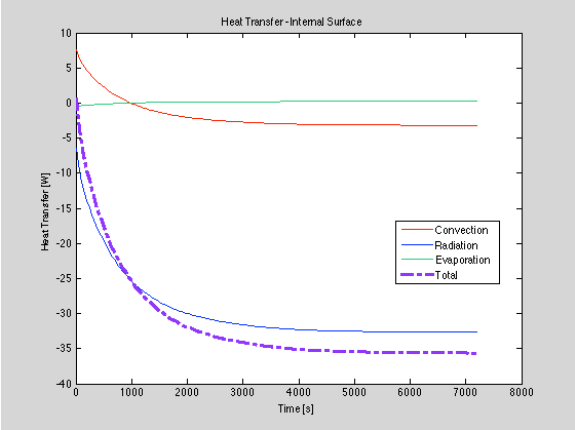

Figure 5 Heat transfer from biomimetic facade

Initially, the convective heat transfer is towards the room, but as the surface temperature decreases over time, the convective heat transfer has a cooling effect on the space. Similarly, radiative heat transfer is initially just above zero, but increasingly has a cooling effect as the perfusion through the façade takes effect.

Temperatures and heat transfer are summarised in Table 4 for the reference and biomimetic cases.

Table 4
Temperatures and Heat Transfer for Biomimetic and Reference Cases

CASE	REF	BIOMIMETIC
Inside surface temperature (K)	300.5	295.9
Inside surface temperature (°C)	27.35	22.75
Heat Transfer (W/m^2)	+16.2	-35.6

DISCUSSION

Referencing Figure 3, in the centre of the façade the temperature stabilises at 287.9 K (14.75°C), heavily influenced by the selection of T_{a0} (water supply temperature) of 287.15 K (14°C). This shows the dominance of the perfusion term in Equation 16. One contributing factor is the heat capacity of water, which is nearly four times greater than the façade matrix material – 4.17×10^6 J/K/m^3 versus 1.14×10^6 J/K/m^3. The water creates a high heat transfer potential of 2.1 kW/K/m^3 of façade volume for the relatively low perfusion rate of 5.0×10^{-4} m^3/m^3/s.

As Figure 3 indicates, the temperature within the biomimetic façade has a parabolic shape with a minimum positioned at x = 0.045m. The relatively flat profile is due to the distribution of water throughout the façade width and is further influenced by the relatively high value of matrix 'tissue' conductivity, k_t. This compares to the linear profile of the conventional façade, which is expected for a static, isotropic material. The differing profiles illustrate a further advantage of the biomimetic façade. While the conventional façade has a temperature differential of 32.4 K, the temperature

difference within the biomimetic façade is limited to 8.0 K.

Figure 3 also shows that internal and external surface temperatures are both higher than the perfusion supply temperature, showing the effect of the boundary conditions. The temperature on the internal surface (295.9 K) is higher than the external surface (292.9 K). Given the high external temperature and solar gain, this result is somewhat counterintuitive, however the fur layer acts as an effective thermal barrier. The conventional façade, without the benefit of a fur layer, has a much higher external surface temperature of 332.9 K.

Figure 4 shows that the internal facade surface temperature is 295.9 K (22.9°C) for the biomimetic case. This is a considerable reduction from the conventional façade at 300.5 K (26.5°C) and affects the occupant thermal comfort as discussed below.

The internal surface temperature of 295.9 K is higher than both the proposed internal air temperature and perfusion temperature, but can be explained due to the radiant heat gains from other room surfaces. From Equation 21, T_{MRT} was assumed to be 301.2 K (28°C). In retrospect, this value of T_{MRT} could be considered too high, given the conventional façade under solar loading resulted in an internal surface temperature of 300.5 K.

From Figure 5, cooling from the biomimetic façade is ~35 W/m^2. This is similar in magnitude to cooling from conventional hydronic systems. Under normal operating conditions, with an internal air temperature of 299.15 K (26°C), Rehau (*Underfloor Heating/Cooling - Technical Information* n.d., p47) suggests cooling output of 35-40 W/m^2. Assuming a 3 K temperature difference and 40 W/m^2 cooling, the required water flow rate would be approximately 3.2×10^{-3} L/s, compared with an equivalent flow rate of 5.0×10^{-2} L/s for the biomimetic system.

Effect on thermal comfort

The model for Predicted Mean Vote, PMV (*ASHRAE Handbook: Fundamentals* 2005, p8.16) can be described by:

$$\mathrm{PMV} = f\left(T_{a,i}, RH, v_i, T_{MRT}, clo, met\right) \qquad (30)$$

The variables $T_{a,i}$, T_{MRT} and v_i are as described previously, while RH is relative humidity, clo is the clothing value of occupant and met is the activity level of occupant (metabolic rate).

In the case of the biomimetic façade, T_{MRT} was affected by the fur and internal perfusion, which reduced the surface temperature. The revised $T_{MRT,bio}$, PMV and PPD results were calculated and are shown in Table 5. Standard summer values for met and clo were assumed (as per *Green Star Technical Manual* 2008, p96). Thermal comfort measures for both the Reference and Biomimetic cases both lie within the preferred range of -0.5 < PMV < 0.5 (*Green Star Technical Manual* 2008, p91). The biomimetic case showed slightly better comfort, with the PMV 0.1 points closer to zero (the 'ideal' comfort level).

Table 5
Temperatures and Heat Transfer for Fur Layer Wall and Reference Cases

	Reference	***Biomimetic***
T_{MRT}	301.05 K	300.25 K
PMV	0.3	0.2
PPD	6.9 %	5.8 %

FURTHER WORK AND PRACTICAL IMPLEMENTATION

There are several opportunities to advance the analysis presented in this paper. The biomimetic model can be further enhanced for summer cooling in terms of wall thickness, façade material properties, cooling fluid, as well as optimisation across the external fur, facade perfusion and evaporative layers. Further investigation of an evaporative layer on the outside of the building may be justified. This would further align the model with that of Gebremedhin and Wu (2001, p539). However, Figure 5 shows that evaporative heat transfer remains near zero throughout the simulation. The potential for evaporative heat transfer exists – following from Equation 12 the evaporative heat transfer is 9.708×10^3 W/m^2/(kg/s). However, due to the psychrometrics, the difference in vapour concentration remains very low (in the order of 10^{-5} kg/m^3). Clearly the perfusion layer presents the dominant biomimetic effect and it may be worthwhile to test the façade performance without evaporative layers.

Pennes' model for bioheat transfer was used in this paper. Alternate models have been devised for bioheat transfer, as described in Charny (1992) and Jiji (2010). For example, the "s-Vessel Tissue Cylinder Model" (Jiji 2010, p323) is based on a range of different-sized blood vessels and tissue geometry. These additional models enable a more detailed translation of biology to technology with control over a wider range of physical parameters.

Furthermore, the proposed biomimetic façade can be physically implemented to understand the engineering limitations and gather empirical data on façade performance. Selecting a matrix material for the perfusion façade is critical to ensure desired cooling fluid flow and dispersion. Envelope materials and sealants are also important. Furthermore, the proposed façade requires cooling water – a potential design concept would connect facades to a hydronic manifold integrated within the HVAC system.

Façade control will also be a technical challenge due to variations in weather, particularly in temperature regions. Facades will be required to function at varying partial loads and variable solar conditions. Feedback control may be suitable, however additional modelling with different external and

internal conditions will aid in refining the control concept.

CONCLUSION

The biomimetic façade model, combining the elements of fur, fluid perfusion and evaporation, was shown to reduce façade surface temperatures when compared to a reference case. The external temperature was reduced by ~40 K while the internal temperature was reduced by 4.6 K. The biomimetic façade provides ~35 W/m^2 of cooling. This is approximately equivalent to a conventional hydronic cooling system. The evaporative component of the system did not contribute to the overall performance.

While the biomimetic façade decreased the inside surface temperature, the effect on mean radiant temperature and occupant thermal comfort was minimal. The biomimetic façade showed only a 0.1 decrease in PMV compared to the reference case.

This study exemplifies how biomimetic concepts can be modelled and simulated to assess thermal performance and occupant thermal comfort. The analysis provides guidance on the application of functional biomimicry for designers and further informs how simulation can influence the building design process. Employing human skin as an example, this investigation demonstrates the potential for biomimicry to provide flexible, adaptive solutions for façade design that provide occupant thermal comfort while minimising energy consumption.

REFERENCES

ASHRAE Handbook: Fundamentals 2005, ASHRAE, Atlanta.

ASHRAE Handbook: Systems and Equipment 2008, ASHRAE, Atlanta.

Technical Manual - Green Star Office Design & As Built Version 3 2008, Green Building Council of Australia.

Underfloor Heating and Cooling n.d., Warma Floor, United Kingdom <www.warmafloor.co.uk>

Underfloor Heating/Cooling - Technical Information n.d., Rehau, Singapore.

Barcroft, H & Edholm, OG 1946, 'TEMPERATURE AND BLOOD FLOW IN THE HUMAN FOREARM', Journal of Physiology, vol. 104, no. 4, pp. 366-76.

Butcher, K (ed.) 1999, Environmental Design - CIBSE Guide A, 6 edn, The Chartered Institution of Building Services Engineers, London.

—— (ed.) 2002, Weather, solar and illuminance data - CIBSE Guide J, The Chartered Institution of Building Services Engineers, London.

Cena, K & Monteith, JL 1975, 'Transfer Processes in Animal Coats. I. Radiative Transfer', Proceedings of the Royal Society of London, Series B, vol. 188, pp. 377-93.

Charny, CK 1992, 'Mathematical Models of Bioheat Transfer', in IC Young (ed.), Advances in Heat Transfer, Elsevier, vol. Volume 22, pp. 19-155.

Davis, LB & Birkebak, RC 1974, 'On the transfer of energy in layers of fur', Biophysical Journal, vol. 14, pp. 249-68.

Deng, Z-S & Liu, J 2004, 'Mathematical modeling of temperature mapping over skin surface and its implementation in thermal disease diagnostics', Computers in Biology and Medicine, vol. 34, no. 6, pp. 495-521.

Gebremedhin, KG & Wu, B 2001, 'A model of evaporative cooling of wet skin surface and fur layer', Journal of Thermal Biology, vol. 26, no. 6, pp. 537-45.

Hammel, HT 1955, 'Thermal Properties of Fur', American Journal of Physiology, vol. 182 no. no. 2 August 1955, pp. 369-76.

Holman, JP 1997, Heat transfer, 8th ed., McGraw-Hill Companies, New York.

Jiji, LM 2009, Heat Conduction - Third Edition, Springer.

Kowalski, GJ & Mitchell, JW 1979, 'An Analytical and Experimental Investigation of the Heat Transfer Mechanisms within Fibrous Media', ASME, Winter Annual Meeting, New York, N. Y., Dec 2-7, 1979, pp. 1-7.

Pennes, HH 1948, 'Analysis of Tissue and Arterial Blood Temperatures in the Resting Human Forearm', Journal of Applied Physiology, vol. 1, no. 2, pp. 93-122.

Scholander, PF, Walters, V, Hock, R & Irving, L 1950, 'Body Insulation of Some Arctic and Tropical Mammals and Birds', Biological Bulletin, vol. 99, no. No. 2, October, pp. 225-36.

Webb, M, Hertzsch, E & Green, R 2011, 'Modelling and optimisation of a biomimetic façade based on animal fur', paper presented to Building Simulation 2011, Sydney, Australia.

Weinbaum, S, Xu, LX, Zhu, L & Ekpene, A 1997, 'A new fundamental bioheat equation for muscle tissue: Part I--Blood perfusion term', J Biomech Eng, vol. 119, no. 3, pp. 278-88.

Wilson, SB & Spence, VA 1988, 'A tissue heat transfer model for relating dynamic skin temperature changes to physiological parameters', Phys Med Biol, vol. 33, no. 8, pp. 895-912.

Wissler, EH 1998, 'Pennes' 1948 paper revisited', Journal of Applied Physiology, vol. 85, no. 1, pp. 35-41.

Xu, F, Lu, TJ, Seffen, KA & Ng, EYK 2009, 'Mathematical Modeling of Skin Bioheat Transfer', Applied Mechanics Reviews, vol. 62, no. 5, pp. 050801-35.